NASA TECHNICAL NOTE

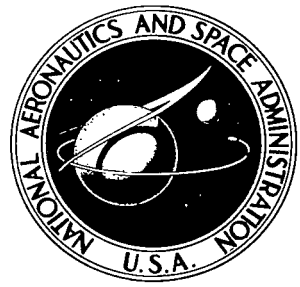

NASA TN D-7038

CONTAMINATION OF SPACECRAFT SURFACES DOWNSTREAM OF A KAUFMAN THRUSTER

by Thaine W. Reynolds and Edward A. Richley

Lewis Research Center
Cleveland, Ohio 44135

NATIONAL AERONAUTICS AND SPACE ADMINISTRATION • WASHINGTON, D. C. • JANUARY 1971

1. Report No. NASA TN D-7038	2. Government Accession No.	3. Recipient's Catalog No.
4. Title and Subtitle CONTAMINATION OF SPACECRAFT SURFACES DOWNSTREAM OF A KAUFMAN THRUSTER		5. Report Date January 1971 6. Performing Organization Code
7. Author(s) Thaine W. Reynolds and Edward A. Richley		8. Performing Organization Report No. E-5913 10. Work Unit No. 120-26
9. Performing Organization Name and Address Lewis Research Center National Aeronautics and Space Administration Cleveland, Ohio 44135		11. Contract or Grant No. 13. Type of Report and Period Covered Technical Note
12. Sponsoring Agency Name and Address National Aeronautics and Space Administration Washington, D. C. 20546		14. Sponsoring Agency Code

15. Supplementary Notes

16. Abstract

Results of experiments to evaluate the effects of thruster exhaust products on surfaces located downstream of two mercury electron-bombardment ion thrusters are presented. It is shown that severe contamination can result from accelerator grid sputtering. The flux of grid sputtered material, though smaller in magnitude than the neutral mercury flow, will readily condense on and not reevaporate from surfaces at temperatures normally expected in near-Earth orbits. Measurements of solar-cell output were used to monitor the deposition rate of material onto the cell surfaces. Metallic deposits, identifiable with grid components by spectrographic analysis, accumulated at rates consistent with calculated deposition rates of sputtered grid material.

17. Key Words (Suggested by Author(s)) Solar cells Ion thrusters Sputtering Contaminant flux	18. Distribution Statement Unclassified - unlimited		
19. Security Classif. (of this report) Unclassified	20. Security Classif. (of this page) Unclassified	21. No. of Pages 29	22. Price* $3.00

*For sale by the National Technical Information Service, Springfield, Virginia 22151

CONTAMINATION OF SPACECRAFT SURFACES DOWNSTREAM OF A KAUFMAN THRUSTER

by Thaine W. Reynolds and Edward A. Richley

Lewis Research Center

SUMMARY

Results of experiments to evaluate the effects of thruster exhaust products on surfaces located downstream of a 30-centimeter- and a 1.5-meter-diameter Kaufman thruster are presented and compared with results from a similar experiment on SERT II. It is shown that severe contamination can result from accelerator grid sputtering. Although smaller in magnitude than the flux of neutral mercury propellant flow, the flux of sputtered grid material readily condenses on and does not reevaporate from surfaces at temperatures normally expected in near-Earth orbit.

In the first experiment, solar cells were located downstream of the thrusters in such a way that their short-circuit current output could be monitored throughout the test. This test provided data on the deposition rate of contaminant at a given location. In the second experiment, strips of glass slides were located in two planes downstream of the thruster. After the test the slides were removed from the facility and the deposition distribution was determined with two optical methods.

The first experiment showed that, when the solar cells were within the main thruster ion beam, they remained clean because of ion resputtering; however, when they were outside the main beam, they became contaminated. The second experiment confirmed that the distribution of contamination ranged from zero near the thruster axis, up to a peak value and then to near zero with increasing radial distance. Based on the extent of the deposition and time of test, it was calculated that the average grid sputtering rate for the 150-centimeter-diameter thruster was about 210 monolayers per hour. Further calculations showed that this sputtering rate would result if about 1 percent of the ion exhaust was in the form of charge-exchange ions that struck the accelerator grid.

Qualitative agreement was found between the deposition rate tests on SERT II and the vacuum facility tests.

INTRODUCTION

Previous reports have pointed out that neutral propellant efflux from electric thrusters may be sufficiently high to cause condensation on surfaces located downstream of the thruster exhaust under some conditions of operation (refs. 1 and 2). The possible problems associated with such fluxes were pointed out - not because they appear formidable, or in any way insurmountable - but because they need to be considered in overall spacecraft design. In a like manner, designers must consider and avoid placing spacecraft components in the principal region of the primary ion beam. Another source of thruster efflux to be considered from the spacecraft design viewpoint is that of the charge-exchange ions formed by interaction of the primary ion beam with the nonionized neutral propellant exhaust. The subject of charge-exchange ion behavior has been reported in references 3 and 4 with regard to possible arrival rates on nonthruster surfaces.

Of equal, and perhaps more serious importance, is still another thruster efflux, that of sputtered accelerator grid material which results from bombardment of the downstream face of the accelerator grid by charge-exchange ions. Because the grid material, be it molybdenum, stainless steel, or any other metal, has a considerably lower vapor pressure than neutral mercury propellant, it may readily condense upon and not reevaporate from surfaces downstream of the thruster. Thus, even though the magnitude of the sputtered grid flux may be lower than that of the neutral mercury flux, it may stick and build up a coating on surfaces under conditions in which mercury generally reevaporates. For example, at locations of less than about 2.5 Earth-orbit radii from the Sun, spacecraft equilibrium surface temperatures would be such that neutral mercury exiting from thrusters would not condense, but sputtered grid material would.

In order to verify experimentally the magnitude and distribution of sputtered grid fluxes, solar-cell modules and plain glass collector surfaces were placed in the vicinity of different thruster exhausts. This report presents the results of these tests. Included among the results are (a) solar cell outputs, (b) transmittance measurements on films, (c) surface conductivity, and (d) spectrographic analysis of coatings on surfaces.

THEORETICAL CONSIDERATIONS

Particle Emission

The exhaust from electrostatic thrusters (as pointed out in refs. 1 and 2) consists of the highly energetic charged particles of the ion beam, somewhat lower energy charge exchange ions, and low-energy neutral particles (sputtered grid metal and nonionized propellant). The magnitude and effects of these various species is reviewed in this section.

Ion beam. - The high-energy ions of the main beam will cause erosion of objects in their paths. This type of encounter must be avoided for the major portion of the beam at least. A study of exhaust beam profile maps from several mercury ion thrusters at Lewis determined that over 96 percent of the primary ion beam exhausted from conventional two-grid accelerator systems is confined within a beam spreading half-angle of 20^{o} (ref. 1). The manner in which the ion beam profile drops off at larger angles has had less attention (refs. 5 and 6). However, since long mission times are being considered for some applications, the long-range effects on surfaces of these peripheral, small beam fractions must be examined. For instance, at a representative thruster ion beam density of 30 amperes per square meter the mercury ion flux rate corresponds to about 15.6 monolayers per second or 1.35×10^{6} monolayers per day of propellant flow. The sputtering capabilities of these high-energy ions is of the order of 1 to 10 atoms per incident ion, depending upon their energy and the material of the target. It is possible, then, to have target sputtering rates of 100 to 1000 monolayers (250 to 2500 Å; 2.5 to 25×10^{-8} m) per day at angles off the beam axis where the beam intensity has dropped to 0.0001 times the thruster exit beam intensity.

Charge-exchange ions. - Analyses of the probable fraction of an ion beam that may be converted to charge-exchange ions have been carried out (e.g., ref. 3). The amount of charge exchange is estimated from

$$f = \sigma_{ce} n x \tag{1}$$

where

f fraction of beam ions converted to charge exchange ions

σ_{ce} charge exchange cross section, cm^2

n neutral atom density, $atoms/cm^3$

x distance over which fraction f conversion occurs, cm

(All symbols are defined in appendix A.)

The charge-exchange ion current is considerably smaller than the main beam current. Its random distribution of direction and energy makes determining its ultimate behavior complicated. However, computer studies have been used to determine, for the case of a 15-centimeter thruster (ref. 3), that, of a total charge-exchange fraction of 0.00327, about 85 percent would be expected to impinge on the downstream side of the accelerator. After impingement this fraction of the current is probably reemitted as neutrals (along with sputtered grid material). Since the creation of the charge exchange ions was at the expense of emitted neutrals initially, this addition to neutral flow essentially effects no change from the original neutral emission rate. The approximately

15 percent of the total charge exchange ion current not assumed to impinge on the accelerator grid may arrive at other spacecraft surfaces and create environmental problems (ref. 4).

Sputtered grid material. - Impinging charge-exchange ions will cause grid erosion through sputtering. Sputtered molybdenum grid material will be ejected downstream of the thruster. The low vapor pressure of the grid material will cause it to adsorb or condense on whatever surface it strikes and to build up a contaminant layer.

Both the magnitude and distribution of sputtered material is affected by the angle of incidence of the impinging ions with the surface and by the incident ion energy (refs. 7 and 8). In general, sputtering efficiency increases at more oblique angles of incidence of impinging ions. Because the sputtering ratio (atoms per incident ion) will be in the range of one to three for the situation being reported, the amount of sputtered grid material is expected to be about one to three times the equivalent charge-exchange ion current.

The distribution of the sputtered material is difficult to predict accurately, because not only is it a function of angle of incidence and energy level of the impinging ions, but also, the grid surface itself is altered in shape throughout the test because of the sputtering erosion. Wehner (ref. 7) found that normally incident ions of energies up to 1000 volts resulted in a sputtering distribution that was "under cosine" (i. e., more material was ejected to the sides than normal to the surface). Between 1000 and 20 000 volts the distribution changes from under cosine to "over cosine."

Musket and Smith (ref. 9) found that the cosine distribution accounted for more than two-thirds of the atoms sputtered by 1- to 10-kilovolt mercury ions. Finally, influences of surface irregularities due to sputter erosion tend toward an over-cosine distribution.

For the calculations herein, a cosine distribution pattern has been assumed. As will be shown later when results are compared with experiment, this simplification permits conservative engineering estimates to be readily made.

Using the cosine distribution relation along with related thruster conditions, one can develop an expression for the envelope of locations of a surface such that the accumulation of deposit on that surface is limited to some predetermined value in a given time.

Let Z be the thickness in monolayers to be permitted to accumulate on a surface at the end of some time limit t. Then,

$$Z = \mu \frac{t}{\sigma_m} \tag{2}$$

where

μ arrival rate of sputtered material, atoms/(cm^2)(sec)

σ_m monolayer concentration, atoms/cm^2

Equation (2) assumes a sticking coefficient of unity. Now

$$\mu = \frac{\mu}{\nu}\nu \tag{3}$$

where ν is the emission rate of sputtered material and μ/ν is the equivalent of a geometric view factor giving the fraction of emitted flux which arrives at a given location. Using far-field relations (ref. 10), the view factor for a surface at a distance L, normal to the incident flux from a thruster of radius R, is

$$\frac{\mu}{\nu} = \frac{\cos\theta}{\left(\frac{L}{R}\right)^2} \tag{4}$$

where θ is the angle between the normal to the thruster emitting surface and the direction line to the receiving surface. The emission rate is

$$\nu = \frac{I}{A}\frac{f}{q}S \tag{5}$$

where S is the sputtering ratio (grid atoms sputtered/incident charge-exchange ion). Combining equations (2) to (5) and solving for L/R give

$$\frac{L}{R} = \left(\frac{\cos\theta}{Z}\frac{I}{A}f\frac{t}{q\sigma_m}S\right)^{1/2} \tag{6}$$

Equation (6) expresses the distance away from a thruster exit that a surface must be located to limit its accumulation of sputtered grid material to a layer thickness Z monolayers in t seconds.

Using the conditions for the thruster analyzed in reference 3 (a thruster typical of those used on the SERT II mission (ref. 11)), and assuming S = 1, reduce equation (6) to

$$\frac{L}{R} = 0.134\sqrt{\frac{t\cos\theta}{Z}} \tag{7}$$

Equation (7) is shown plotted in figure 1 for various times with Z = 20. If, for example, one wishes to limit the accumulation on a solar-cell array to 20 monolayers (at which thickness the light intensity to the cell would be lowered to about 60 to 70 percent of its value without a deposit), then figure 1 gives the envelope of curves showing the distance away that surfaces must be located for any particular time period. No beam resputtering of the deposit is assumed with this plot.

Neutral atom efflux. - The quantitative analysis of the magnitude and possible effects of neutral mercury atom efflux from bombardment thrusters has been considered in detail (refs. 1 and 2). As noted in these references, at the present levels of thruster current density and propellant utilization efficiency, condensation of mercury will not occur on surfaces at temperatures much above the 200 to 210 K range.

In the present experiment, surface temperatures are too high to permit any bulk condensation of mercury. However, it is possible that fractional monolayer amounts may adsorb on surfaces because of the high desorption energies observed at low coverages of mercury (ref. 12). It also seems possible that, with freshly sputtered grid material continually being deposited on a surface, the simultaneous arrival of grid material and neutral mercury atoms could cause some continual mercury adsorption. No such behavior as this has reportedly been observed, however.

Thin Films

The behavior of thin films of materials with respect to their light transmission and electrical properties is an extensive subject area. Only a cursory discussion is presented here for the purpose of establishing the order of magnitude of film thicknesses involved in the measurements that were made.

Light transmission. - Transmission of visible light through films of silver (Ag) and aluminum (Al) are shown in figure 2. Data are from reference 13. Some variation in film structure was evidently obtained, depending on the rate of formation of the film. For these films a 50-percent decrease in light transmission was obtained for films of around 70 Å (0.7×10^{-8} m) thickness (approx. 30 monolayers for Ag or Al).

The transmittance of films is, of course, frequency dependent. The deleterious effects of a film deposit, then, may be different for an instrument or experiment sensitive only to visible wavelength light from what it would be for one which has a broader range of sensitivity (such as solar cells, which have greater sensitivity in the infrared region). A comparison of transmittance values for some of the films formed herein will be shown in the section EXPERIMENTAL RESULTS.

Electrical conductivity. - Considerable variation in the resistivity-film thickness relation has been observed for metal films. Some curves for silver and gold films on glass (ref. 13) and for an alkali film (ref. 14) are shown in figure 3. One can note from

this figure that there is generally a rapid change in resistivity with film thickness below film thicknesses of about 100 Å (10^{-8} m).

The reactivity of freshly formed thin films on exposure to air causes changes in the chemical composition and hence changes in electrical characteristics. Resistance measurements alone, then, do not appear to be a reliable guide to film thickness determinations for very thin films. Such measurements may be of interest, however, because of the possible effects of such conducting films on system behavior.

EXPERIMENTAL SETUP AND PROCEDURE

The experimental setup reported on herein is shown in figure 4. The vacuum tank facility is 7.6 meters in diameter by 22 meters long. The thrusters used in this series of tests were a 1.5-meter-diameter thruster using 10 oxide cathodes (ref. 15) and a 30-centimeter-diameter hollow cathode thruster (ref. 16). A panel containing four solar-cell modules (fig. 5) was mounted in the tank as also shown in figure 4. These were silicon solar cells with a protective glass cover. Some experimental and geometric parameters pertinent to the setup are given in table I.

When either thruster was being operated, the solar-cell outputs could be monitored to see if any efflux from the thruster was affecting their performance. It should be noted here that this solar-cell experiment was a "piggyback" one. That is, the thruster operation was scheduled for tests other than this contamination experiment. Results from the tests are therefore reported principally on a basis of thruster operating time only, with no control being exercised over the variation in thruster parameters during this operating time.

The source of illumination used for the cells was a tungsten-iodine wide floodlamp mounted outside the tank and directed toward the solar-cell panels through a quartz window (fig. 6). A single reference solar cell was mounted on a rotatable, retractable shield as shown in figure 6. The reference cell was extended to the position shown and the lamp power set to give a selected value of short-circuit current from the reference cell. The shield was then rotated out of the way and retracted so that the experimental cell outputs could be measured. After the readings were taken, the lamp was shut off and the shield pulled up into the window well to protect the window from any back-sputtered tank material.

The variable measured as an indication of surface contamination of the main cells was the short-circuit current, since this is the parameter that is directly related to the amount of light reaching the cell.

Another means used for checking for surface contamination was to monitor the electrical resistance between two points on the surface. These surface resistance probes are shown on two of the modules in figure 5.

A second phase of the experiment was directed at obtaining information on the distribution of material sputtered from the grids. To do this, an array of glass collector slides was placed in the facility as shown in figure 7. The slides were mounted onto stainless steel strips which in turn were hung from metal cables strung across the tank diameter at two axial locations, 2.28 and 4.1 meters from the thruster exit. The array thus covered a range of radial distances and angles from the thruster in two quadrants of the tank. The 1.5-meter thruster was operated for a total of about $6\frac{3}{4}$ hours. The slides were then removed from the tank and checked for light transmission and electrical conductivity.

For the glass collector phase of the experiment the thruster was operated specifically for this test. The average beam current was 11 amperes, and the total equivalent mercury flow was $16\frac{1}{3}$ amperes, giving an average propellant utilization efficiency of 0.67. At the voltages used, the sputtering ratio S of stainless steel (the grid material) was estimated at 3 atoms per incident mercury ion from the data of reference 17.

EXPERIMENTAL RESULTS

Deposit Rate

The results of some of the solar-cell experiments are shown in figures 8 and 9. Figure 8(a) shows the typical behavior of the short-circuit current output of one solar-cell module during the course of 30 hours of operation of the 1.5-meter thruster. The behavior was typical of all the cells during several different thruster operating periods. Since the short-circuit current is directly related to the light received by the cells, the drop in output current is related to the thickness of the deposit being laid down on the cell covers. Figure 8(b) shows the surface resistance measured during the 1.5-meter-thruster run. The range of resistance shown (10^3 to 3×10^6 ohms/square) was the measurable range of the circuit used. The thicker films had resistances below the 10^3 ohm range.

In figure 9 are shown typical curves of the short-circuit current output of the cells during operation of the 30-centimeter thruster. This run did not immediately follow the 1.5-meter run shown in figure 8. Therefore the values of current ratio I/I_o at the start of the 30-centimeter run do not start at the values occurring at end of the 1.5-meter run cited.

Comparison of figures 8 and 9 indicates that material was being deposited on the cell covers during operation of the 1.5-meter thruster, but was being removed during operation of the 30-centimeter thruster. It will be noted from the layout in figure 4 that the solar cells are located closer to the axis of the beam of the 30-centimeter thruster than they are for the 1.5-meter thruster. The 30-centimeter thruster beam density at

the solar-cell locations is apparently sufficient to sputter off the deposited material which is accumulated during operation of the larger thruster. Figure 9 shows that in the first 2 hours cells C and D (which were closer to the beam) were cleaned off more rapidly than cells A and B, which were farther away from the beam axis.

Samples of the coating material were removed from the solar-cell covers by being dissolved in dilute nitric acid. Spectrographic analyses of these samples identified the following elements: chromium, copper, iron, molybdenum, nickel, lead, silicon, tin, and traces of titanium and zinc. These elements are identifiable with thruster components. In particular, it is to be noted that the accelerator grid of the 1.5-meter thruster is made of stainless steel (chromium, iron, nickel, silicon, and molybdenum).

The solar-cell cover temperatures ranged from 0° to 150° F. The high-temperature levels did not lessen the accumulation rate, nor did the deposit evaporate at this level. The implication from these observations is that no mercury adsorption was occurring during the course of the run. The deposit is all material with relatively low vapor pressure.

Deposit Distribution

In the second phase of the experiment, the strips containing the glass collector slides were removed from the tank after the thruster had been operated for $6\frac{3}{4}$ hours. After the transmittance and conductivity measurements were made, the slides were remounted on boards to simulate their arrangement in the tank.

Photographs of these remounted slides are shown in figure 10. One can readily note the distribution pattern of the deposited material in figure 10(a), for example. The essential features of the pattern are obvious. At small angles from the thruster edge (less than about 15°), the slides remain free of deposit. At larger angles film deposition starts to build up, reaches a maximum thickness in the neighborhood of 30°, and then decreases in thickness at larger angles.

This behavior is readily anticipated from the following considerations (sketch (a)).

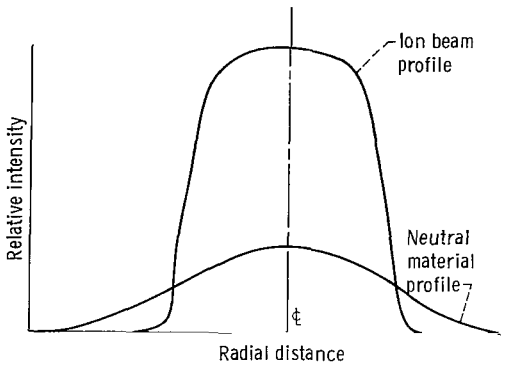

(a)

The ion beam profile at any axial location is high in the central core and drops off sharply starting at some radial location (refs. 5 and 6). The profile of neutral sputtered grid material, assuming random emission from the grid, has the familiar cosine distribution pattern associated with such a random source.

A surface located in the thruster wake will remain free of deposit at any location where the sputtering rate caused by arriving ions is greater than the arrival rate of condensable neutral atoms ($jS/q \geq \mu$). Close to the thruster edge, then, the ion beam intensity is still high enough to resputter any grid material which might condense. The ion beam density drops off much more rapidly than the neutral density, however. At some radial location, where the arrival rate μ becomes greater than the sputtering rate $[(j/q)S]$, grid material will start to deposit on a surface. The net deposition rate $[\mu - (j/q)S]$ will increase with increasing radial distance up to some point beyond which it will decrease since the arrival rate of sputtered material must approach zero at large radial distances.

Transmittance measurements. - The transmittance through the films on the glass slides were checked on a simple bench setup using a silicon solar-cell detector and the same tungsten lamp source described previously. Since the solar-cell detector is sensitive to light wavelengths from about 3000 to 11 000 Å (0.3 to 1.1 μm), it was felt desirable to compare the transmittance values so obtained with those obtained with a microphotometer.

One complete strip of slides which covered the widest variation in deposit thickness was therefore also run on a microphotometer with a photomultiplier detector sensitive to wavelengths from about 3000 to 6500 Å (0.3 to 0.65 μm). The comparison of these two sets of measurements is shown in figure 11. Transmittance values with the solar-cell detector are in general a little higher. However, the values and trends are sufficiently similar, so that no further comparisons seemed necessary for the present inves-

tigation. Transmittance values cited hereafter were determined with the solar-cell detector.

Transmittance values through all the slides are shown in figure 12. At the near plane (fig. 12(a), at 2.28 m) the slides within about 18° of the thruster edge remained free of deposit. Maximum deposit thickness (indicated by minimum transmittance) occurred around 34° to 36°. Beyond 36° the deposit thickness decreased to essentially zero at the tank wall.

At the downstream plane (figs. 12(b) and (c) at 4.1 m) the slides within 12° of the thruster edge are free of deposit (strip B). Strip D at this plane location appears to be anomalous in behavior compared to the other strips. There were metal obstructions in the tank close to this strip which may have contributed to this situation. Because of this, the data obtained on strip D have been ignored in the remaining discussion.

In order to get an estimate of the thickness of the deposited layer, the transmittance values were used in conjunction with the transmittance - film-thickness curve for 75-minute deposition time for Ag (fig. 2). The resulting film thickness values for strips A and B are shown in figure 13. Also shown in this figure for comparative purposes are calculated curves for the total deposit that would be collected if no beam resputtering occurred, and if a 3200 Å (32×10^{-8} m) layer of grid material were emitted in a cosine pattern. The view factor equation leading to the calculated curve is (ref. 10)

$$\frac{\mu}{\nu} = \frac{1}{2}\left\{1 - \frac{\left(\frac{L}{R}\right)^2 + \left(\frac{r}{R}\right)^2 - 1}{\sqrt{\left[\left(\frac{L}{R}\right)^2 + \left(\frac{r}{R}\right)^2 + 1\right]^2 - 4\left(\frac{r}{R}\right)^2}}\right\} \tag{8}$$

The data are not extensive enough to determine the distribution of emitted material. However, flux appears to be dropping off more rapidly at wider angles than a cosine distribution would imply. Thus, as noted in the section Charge-exchange ions, the assumption of a cosine distribution for calculational purposes leads to conservative predictions which should be useful for engineering design estimates. Assuming a cosine pattern, the data from strips at both downstream planes lead to essentially the same indicated value of total emission, namely, about 3200 Å (32×10^{-8} m) or an equivalent grid sputtering rate of about 210 monolayers per hour.

The amount of grid material sputtered due to charge-exchange erosion may be estimated from

$$\nu_s = \frac{I}{A}\frac{f}{q}\frac{S}{\sigma_m}(3600) \tag{9}$$

where

ν_s rate of grid sputtering, monolayers/hr

I ion beam current, A

A thruster cross-sectional area, cm^2

f fraction of ion beam converted to charge exchange

q charge per ion, 1.6×10^{-19}

S sputtering ratio, atoms sputtered/incident ion

σ_m monolayer coverage for grid material, $atoms/cm^2$

Using the values I = 11 amperes, A = 1.77×10^4 square centimeters, S = 3, $\sigma_m = 1.93\times10^{15}$ (mean value for iron), and ν_s = 210 monolayers per hour, a value is obtained for f = 0.0094. That is, nearly 1 percent of the ion beam was converted to charge-exchange ions, which caused erosion of the grid material.

Beam profile. - The transmission curves (e.g., fig. 12(a) and (b)) indicate that the ion beam is essentially confined to within about 16° of the thruster edge. This fact was also confirmed by some ion beam surveys taken by a traversing probe located approximately 1 meter downstream of the thruster exit. One such survey map, typical of those taken, is shown in figure 14. The ion beam was reasonably symmetric, although it appears to be directed a few degrees off axis (compare the constant current density contours to the thruster diameter curve). The normalized beam density profile shows that the current density has dropped to very low values beyond about 10° from the thruster edge.

The beam current density profile in this region where deposit formation begins could be estimated from data such as shown in figure 13. The difference between the dashed curve μ and the solid curve $[\mu - (j/q)S]$ represents the amount of material resputtered $[(j/q)S]$ by the ion beam "wing," that is, the very low density edges of the beam. Knowledge of the appropriate sputtering ratio S, therefore, permits an estimate of the current density j.

Noting that μ just equals $[(j/q)S]$ at the location where deposit formation starts, one can combine this fact with equations (3) to (5) to obtain the result

$$\frac{j}{j_o} = f\frac{\cos\theta}{\left(\frac{L}{R}\right)^2} \tag{10}$$

where j_o is the average current density of the thruster. Since $f \leq 0.01$ generally, and each of the other terms of equation (10) contributes to further decreasing the value of the

expression, the conclusion is that when grid material starts to form on a surface at some angle away from the thruster centerline, the ion beam density at that point is considerably less than 1 percent of the main beam density.

Film resistance. - The resistance curves of thin films show too much variation with film thickness to be used as a reliable guide to thickness determination. (Some typical curves found in the literature are shown in fig. 3.) Nevertheless, the resistance range measured for the deposits encountered in these experiments may be of interest.

Figure 15(a) shows plots of the resistance against transmittance for the solar-cell experiment data of figure 8. These resistance values were measured in place, as described in the section EXPERIMENTAL SETUP AND PROCEDURE.

Figure 15(b) shows film resistance data for the deposits on the slides which were in the plane nearest the thruster exit. These resistance values were measured after the slides had been removed from the tank.

Comparison of the range of resistance measured in the present study with the curves in figure 3 indicates only that the film thicknesses are probably less than 120 Å (1.2×10^{-8} m).

COMPARISON WITH FLIGHT EXPERIMENT

Results of an experiment on the SERT II spacecraft to detect surface contamination by mercury ion thruster effluents are discussed in reference 18. It is of interest to compare the results of this flight experiment with those of the present report.

Two solar-cell contamination sensors were located near the exhaust plane of each of two 15-centimeter-diameter mercury bombardment thrusters in the flight experiment (fig. 16). The performance of these sensors during the first 30 hours of operation of each thruster is shown in figure 17. The solar-cell performance curve of figure 8 obtained during the operation of the 1.5-meter thruster is also shown for comparison in figure 17.

There were several differences in operating parameters between the two experiments which probably make any detailed comparisons in performance meaningless. For example, startup procedures, operating current densities, voltages, and acceleration grid material differed. The geometric view factors, however, were similar in spite of the large differences in thruster size. The slow initial drop in transmittance observed in the present experiment may be due to the starting conditions, where the ion beam was on for a considerably smaller fraction of the elapsed time as a result of initial arcing problems.

The difference in contamination rates between the high- and low-temperature sensors of the flight experiment probably is due to the higher localized grid sputtering rate

in the region of the neutralizer. (The high-temperature sensor contaminated more rapidly in spite of a slightly lower view factor from the total grid area.)

In general, the solar-cell contamination results from these tests have shown similar behavior. The output of the solar cells decayed to 50 percent of their starting value within 6 to 12 hours of thruster startup. Beyond this time range decay continues in some apparently exponential manner with time, as might be anticipated from Bouguer's law of absorptance (ref. 19).

The 50-percent transmission level corresponds to deposit thickness of about 70 Å (10^{-10} m) (fig. 2). If this thickness collects in 6 to 12 hours on surfaces with view factors of 0.0165 to 0.0172 from a source, then the source emission rate indicated is in the range of 150 to 300 monolayers per hour. The average sputtered grid emission rate determined from the glass slide collection data was about 210 monolayers per hour.

CONCLUDING REMARKS

Results of the experiments reported herein have indicated that the grid material of operating ion thrusters is being sputtered away at rates up to about 300 monolayers per hour (averaged over the total thruster cross-sectional area). The results correlated reasonably well with those from an experiment on an operating spacecraft.

No evidence of mercury adsorption was detected at the condition of the experiment. Bulk condensation of mercury was not expected, but simultaneous grid-metal-mercury adsorption was thought to be a possibility.

Since the sputtered grid material is apparently being distributed nearly randomly from the accelerator surface, it can condense on any surface which would have line-of-sight view to the thruster exit. Simple shielding may be a solution to this problem. However, designs must take into account the possibility of sputtering and/or reevaporation of contaminants from the shield itself.

Surfaces within small angles from the thruster edge - 15° or less - will remain uncoated because of ion beam resputtering. Such surfaces would themselves, of course, also be sputtered by the ion beam. Surfaces located at larger angles than about 15° would probably accumulate deposit. In the tests herein this occurred at a rate such as to reduce light transmission by 50 percent in 12 hours or less. The deposit rate is then a function of the sputtering rate of the grid, the view factor, and the ion beam density at the surface location.

Lewis Research Center,
National Aeronautics and Space Administration,
Cleveland, Ohio, October 2, 1970,
120-26.

APPENDIX - SYMBOLS

A	area, cm^2
f	fraction of beam ions converted to charge-exchange ions
I	current, A
j	current density, A/cm^2
j_o	average thruster current density, A/cm^2
L	distance, cm
n	neutral atom density, $atoms/cm^3$
q	unit charge, 1.6×10^{-19} C
R	thruster radius, cm
S	sputtering ratio, atoms sputtered/ incident ion
t	time, sec
x	distance, cm
y	distance, cm
Z	thickness, monolayers
z	distance, cm
θ	angle, deg
μ	arrival rate, $atoms/(cm^2/sec)$
ν	leaving rate, $atoms/(cm^2/sec)$
ν_s	grid sputtering rate, monolayers/hr
σ_{ce}	charge-exchange cross section, cm^2
σ_m	concentration of a monolayer, $atoms/cm^2$

REFERENCES

1. Reynolds, Thaine W.; and Richley, Edward A.: Distribution of Neutral Propellant From Electric Thrusters Onto Spacecraft Components. NASA TN D-5576, 1969.
2. Hall, David F.; Newman, Brian E.; and Womack, James R.: Electrostatic Rocket Exhaust Effects on Solar-Electric Spacecraft Subsystems. Paper 69-271, AIAA, Mar. 1969.
3. Staggs, John F.; Gula, William P.; and Kerslake, William R.: The Distribution of Neutral Atoms and Charge-Exchange Ions Downstream of an Ion Thruster. Paper 67-82, AIAA, Jan. 1967.
4. Anon.: A Study of Cesium Exhaust From an Ion Engine and Its Effects Upon Several Spacecraft Components. Hittman Assoc., Inc., HIT-399, June 26, 1969.
5. Byers, David C.: Angular Distribution of Kaufman Ion Thruster Beams. NASA TN D-5844, June 1970.
6. Ogawa, H. S.; Cole, R. K.; and Sellen, J. M., Jr.: Measurements of Equilibration Potential Between a Plasma "Thrust" Beam and a Dilute "Space" Plasma. Paper 69-263, AIAA, Mar. 1969.
7. Wehner, G. K.; and Rosenberg, D.: Angular Distribution of Sputtered Material. J. App. Phys., vol. 31, no. 1, Jan. 1960, pp. 177-179.
8. Wehner, Gottfried: Influence of the Angle of Incidence on Sputtering Yields. J. App. Phys., vol. 30, no. 11, Nov. 1959, pp. 1762-1765.
9. Musket, Ronald G.; and Smith, Harold P., Jr.: Competition Between Random and Preferential Ejection in High-Yield Mercury-Ion Sputtering. J. App. Phys., vol. 39, no. 8, July 1968, pp. 3579-3586.
10. Reynolds, T. W.; and Richley, Edward A.: Free-Molecule Flow and Surface Diffusion Through Slots and Tubes - A Summary. NASA TR R-255, 1967, p. 1.
11. Kerslake, William R.; Byers, David C.; and Staggs, John F.: SERT II Experimental Thruster System. Paper 67-700, AIAA, Sept. 1967.
12. Swanson, L. W.; Bell, A. E.; Hinrichs, C. H.; Crouser, L. C.; and Evans, B. E.: Literature Review of Adsorption on Metal Surfaces, Volume I. Final Report 1 May 1966 to 2 July 1967. Field Emission Corp., McMinnville, Oreg. (NASA CR-72402), 1967.
13. Holland, L.: Vacuum Deposition of Thin Films. Wiley, 1956.

14. Mayer, H.: Recent Developments in Conduction Phenomena in Thin Metal Films. Structure and Properties of Thin Films. C. D. Neugebauer, J. B. Newkirk, and D. A. Vermilyen, eds., John Wiley & Sons, Inc., 1959, pp. 225-252.

15. Nakanishi, S.; and Pawlik, E. V.: Experimental Investigation of a 1.5-Meter Diameter Kaufman Thruster. Paper 67-725, AIAA, Sept. 1967.

16. Bechtel, Robert T.: Performance and Control of a 30-Centimeter Diameter Low Impulse Kaufman Thruster. J. Spacecraft and Rockets, vol. 7, no. 1, Jan. 1970, pp. 21-25.

17. Wehner, G. K.; and Rosenberg, D.: Mercury Ion Beam Sputtering of Metals at Energies 4-15 keV. J. App. Phys., vol. 32, no. 5, May 1961, pp. 887-890.

18. Staskus, John V.; and Burns, Robert J.: Deposition of Ion Thruster Effluents on SERT II Spacecraft Surfaces. NASA TM X-2084, 1970. (Also paper 70-1128, AIAA, Sept. 1970.)

19. Allen, William H., ed.: Dictionary of Technical Terms for Aerospace Use, First ed. NASA SP 7, 1965, p. 41.

TABLE I. - VARIABLES OF DEPOSITION

RATE EXPERIMENT

[See fig. 4.]

Parameter	Operation of 1.5-m thruster	Operation of 30-m thruster
Thruster radius, R, m	0.75	0.15
Beam current density, A/m^2	5.7	20.0
Distance from thruster exit to experimental solar cells, L, m	4.2	1.0
Distance to radius ratio, L/R	5.6	6.4
Angle from thruster centerline to solar cell experiment, deg	57.0	39.0
View factor; ratio of flux arriving at solar cell to flux leaving	0.017	0.019

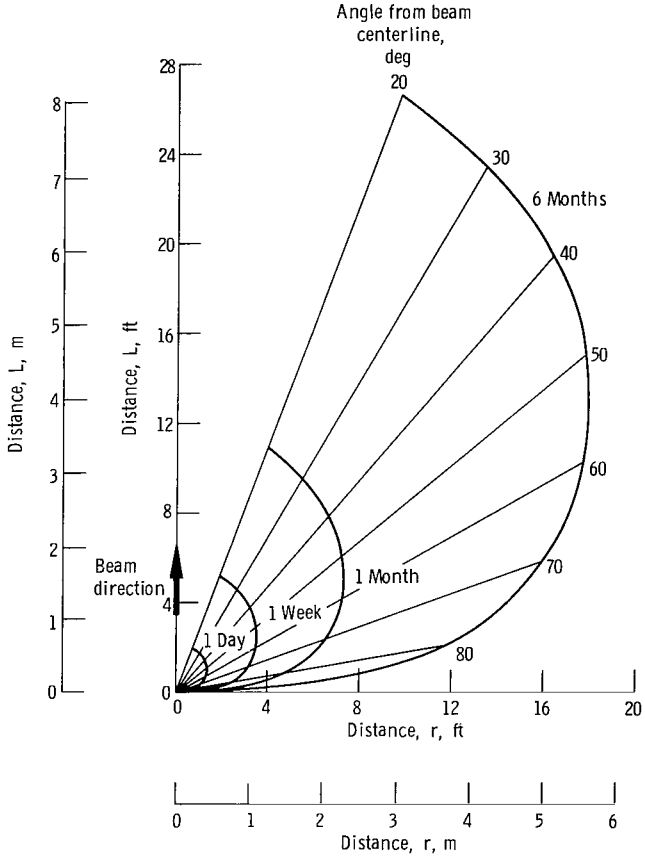

Figure 1. - Envelope outside of which surface must be located to limit accumulation of sputtered grid material to 20 monolayers in time indicated. Thruster diameter, 15 centimeters; sputtering ratio, 1; no ion beam resputtering assumed.

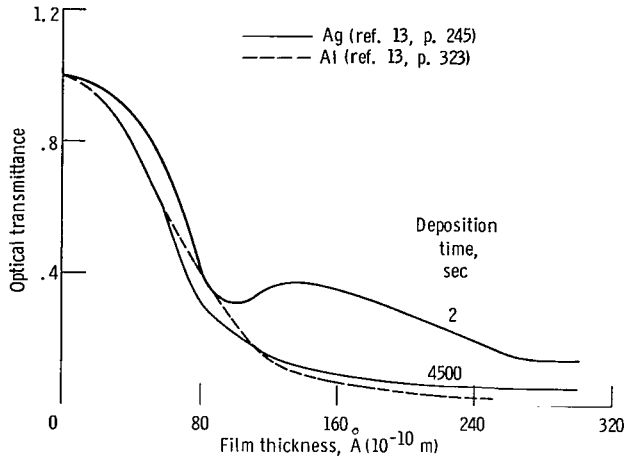

Figure 2. - Optical transmittance of 6500-Å (65×10^{-8} m) light through films of various thicknesses.

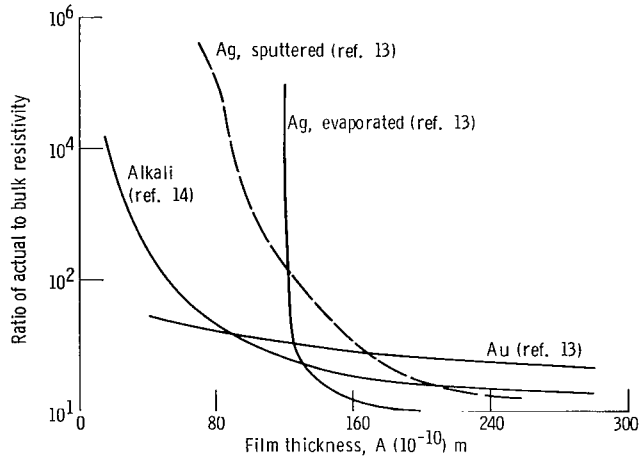

Figure 3. - Electrical resistivity of thin metal films.

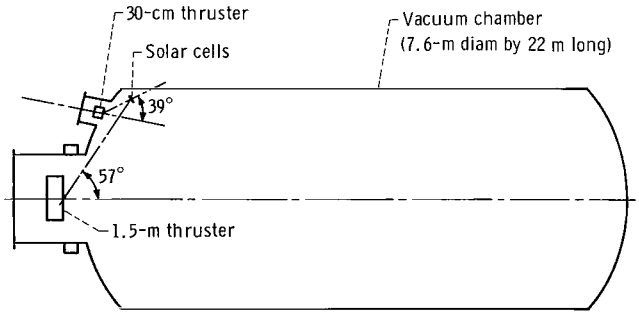

Figure 4. - Schematic layout of solar-cell experiment.

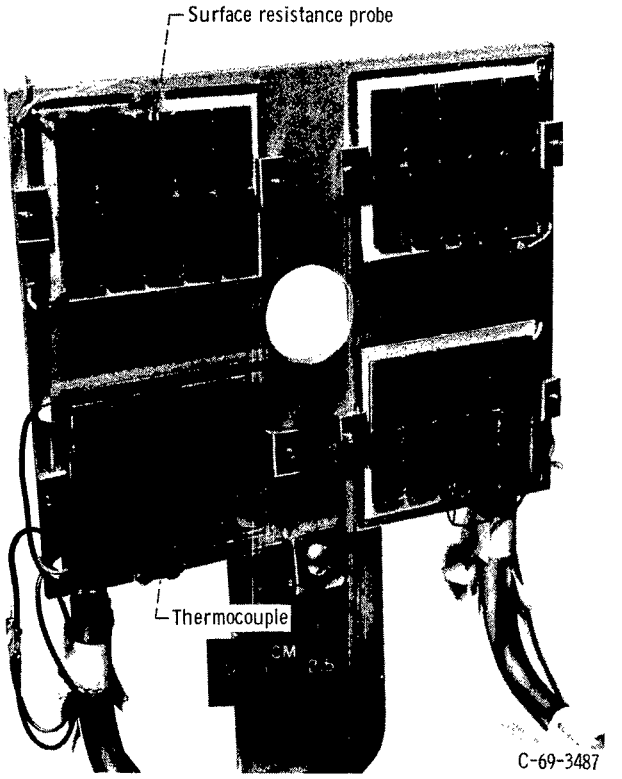

Figure 5. - Experimental solar panels.

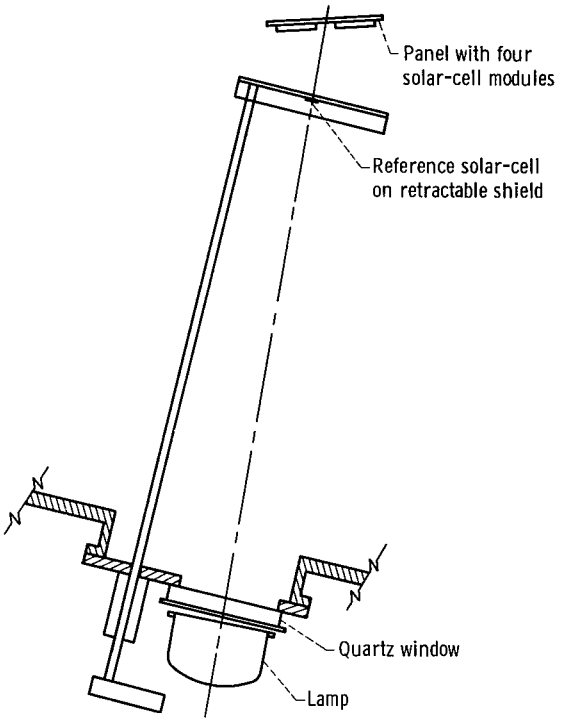

Figure 6. - Layout of solar-cell measuring experiment.

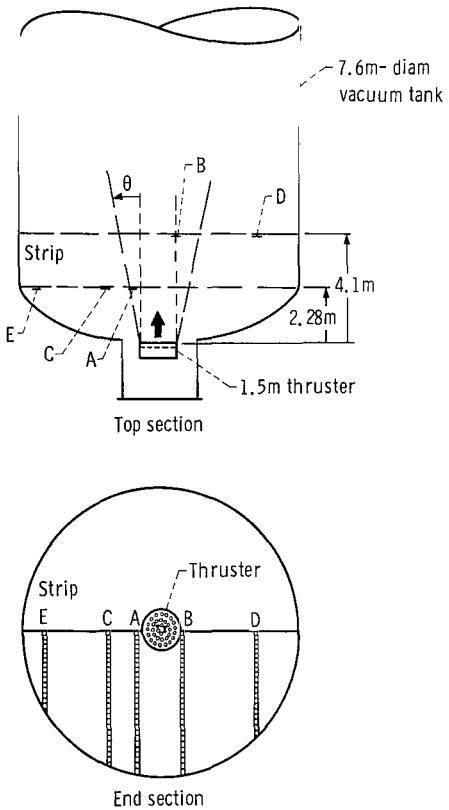

Figure 7. - Location of glass collector strips.

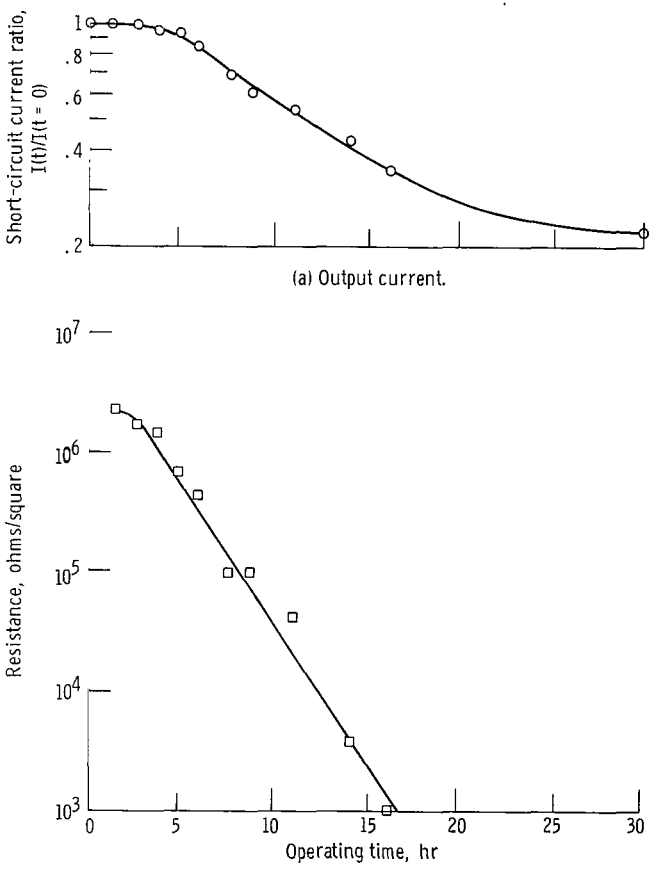

Figure 8. - Typical solar-cell behavior during operation of 1.5 meter thruster.

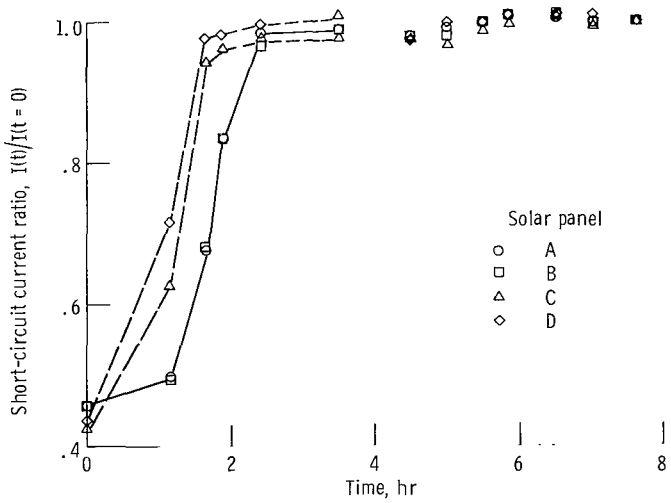

Figure 9. - Typical solar-cell behavior during operation of 30-centimeter thruster.

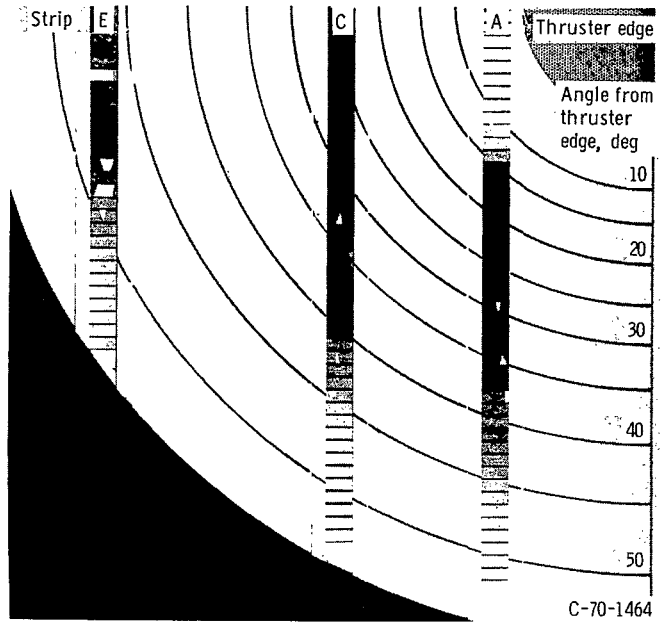

(a) 2.28 Meters downstream; third quadrant.

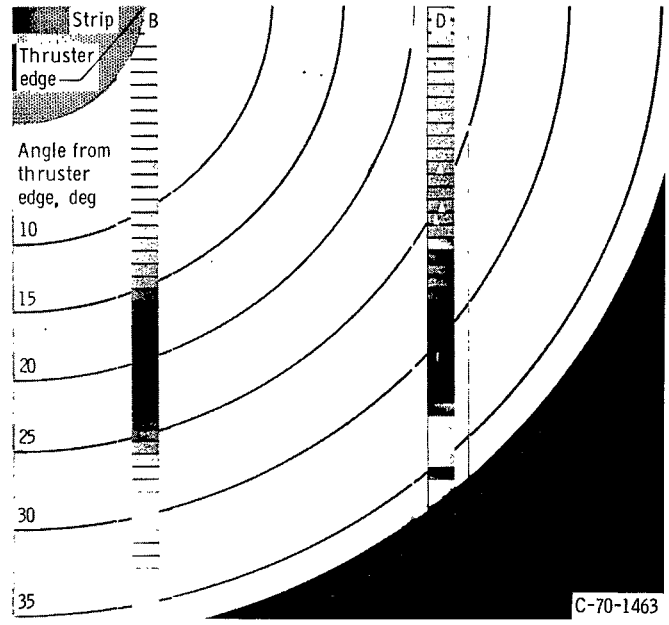

(b) 4.1 Meters downstream; fourth quadrant.

Figure 10. - Reconstructed view, looking downstream from thruster location, of glass slides showing deposit of sputtered grid material. (White spots on strips are areas of glass slide broken in handling.)

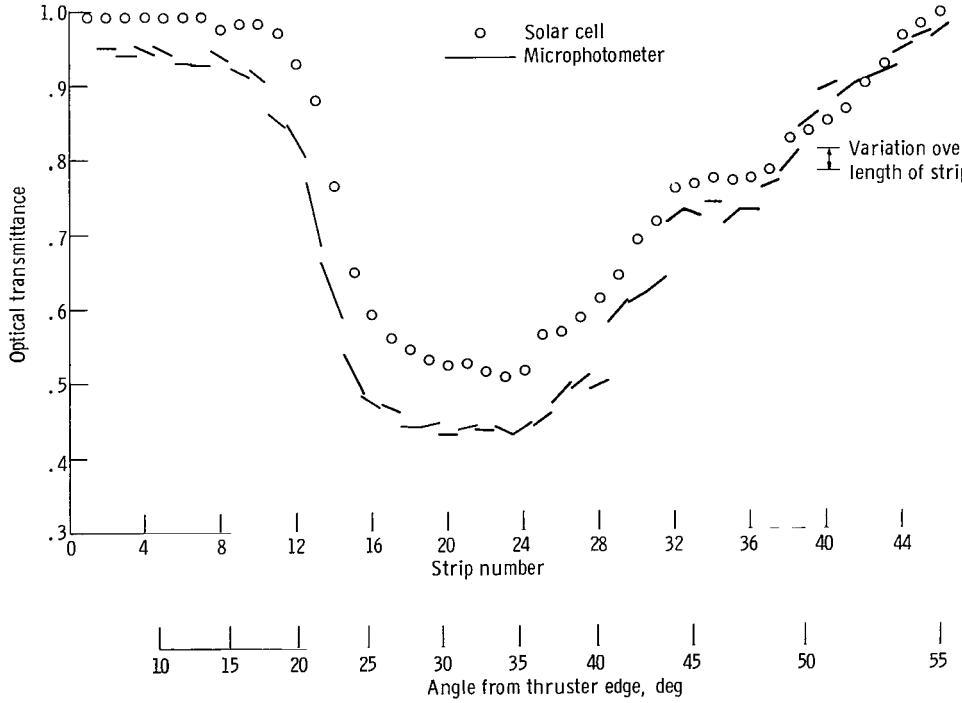

Figure 11. - Comparison of transmittance measurement with solar cell and with microphotometer. Strip A.

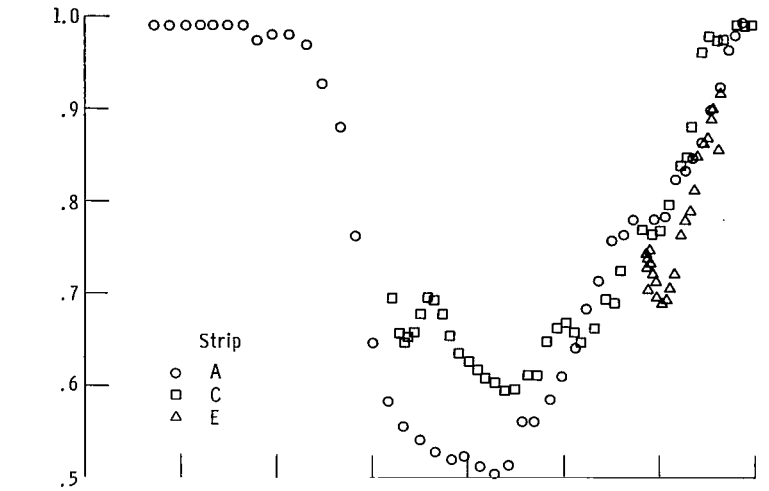

(a) 2.28 Meters downstream.

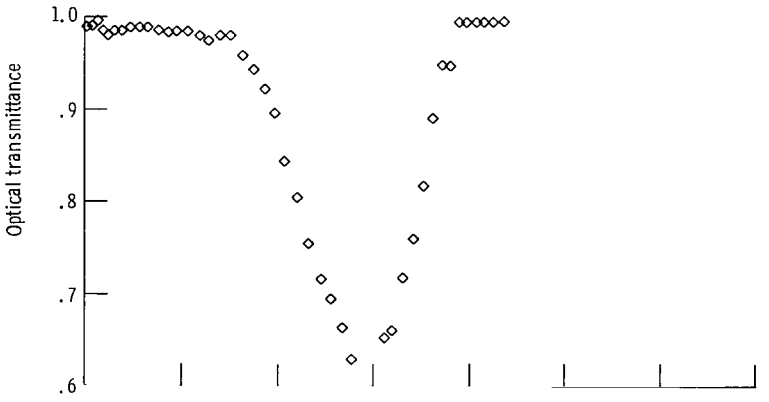

(b) 4.1 Meters downstream; strip B.

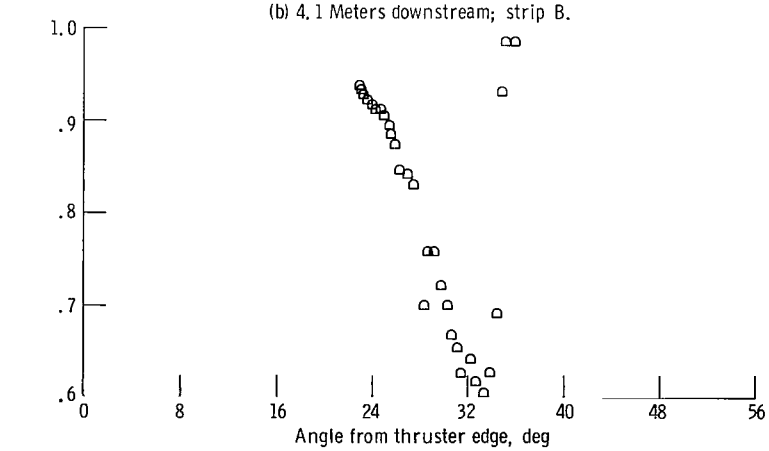

(c) 4.1 Meters downstream; strip D.

Figure 12. - Light transmission through deposit on collector slides

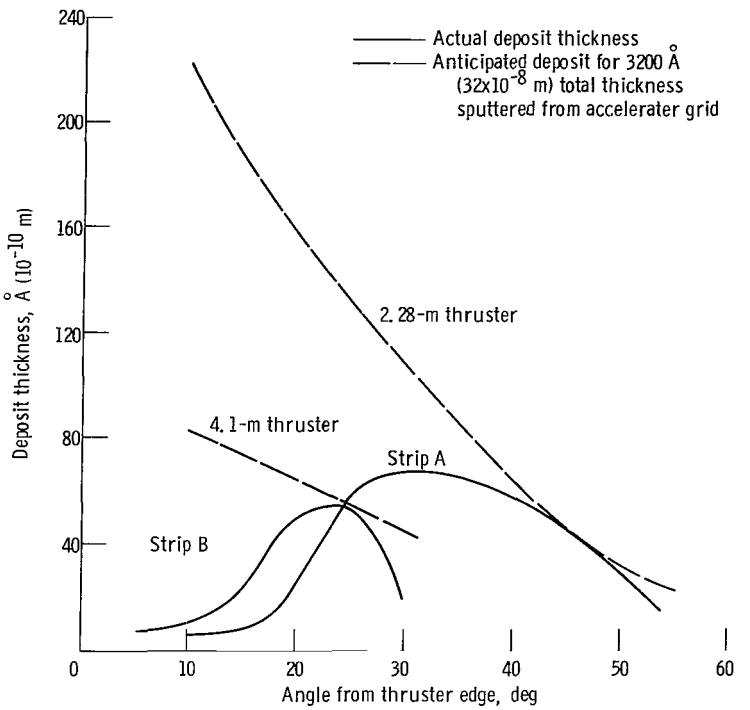

Figure 13. - Variation of deposit thickness with angle from thruster edge.

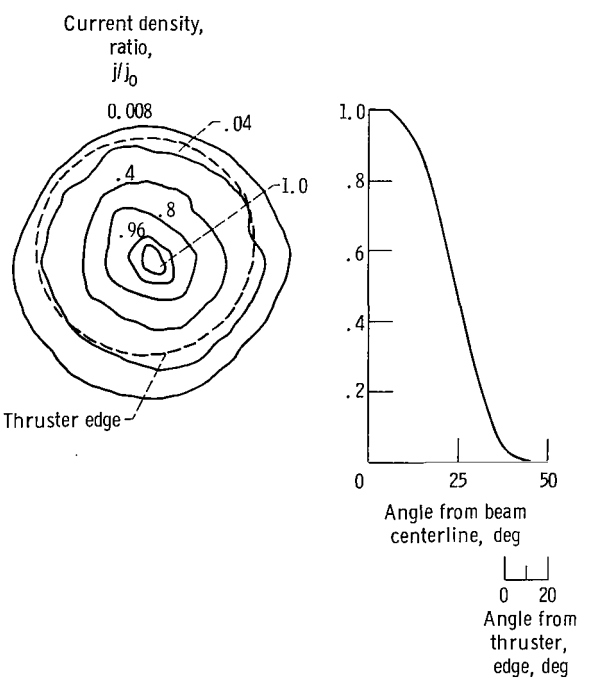

Figure 14. - Ion beam profile survey, 1 meter downstream.

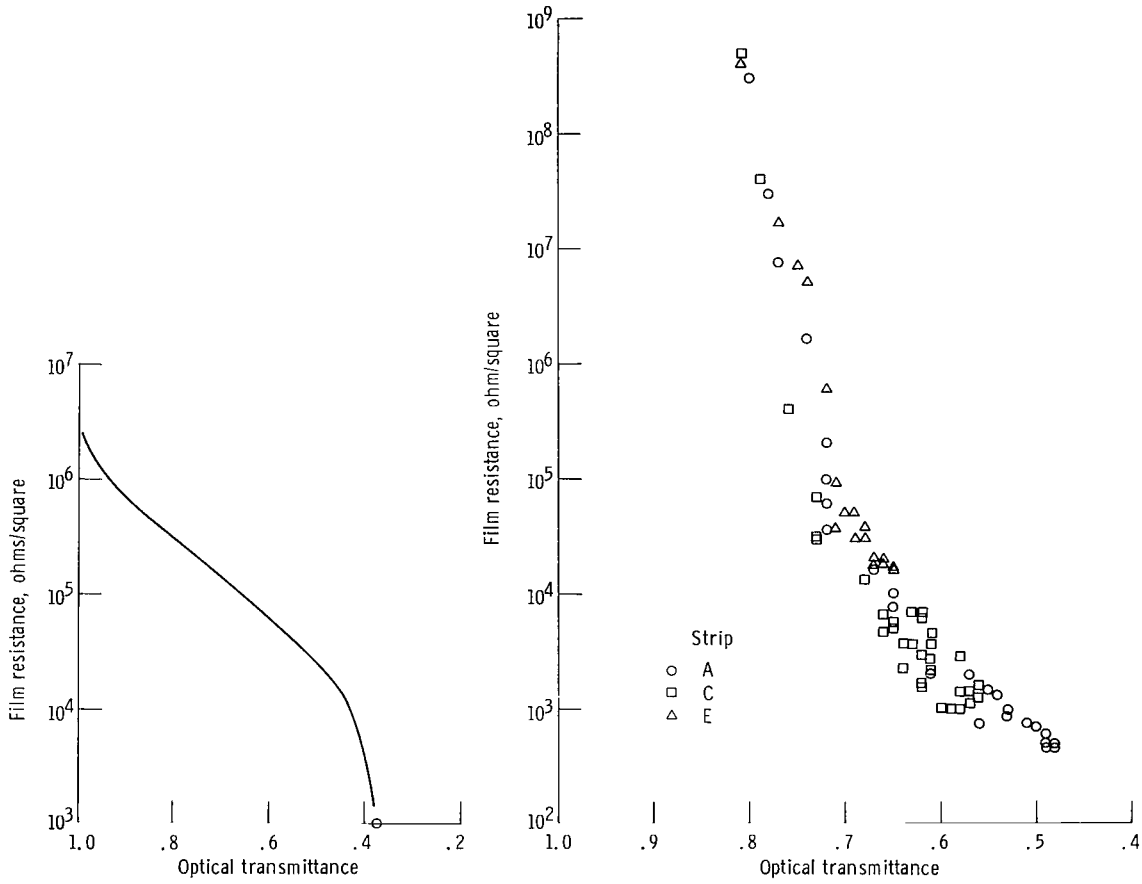

(a) Data from run plotted in figure 8.

(b) Data from run plotted in figure 12(a).

Figure 15. - Film resistance measured on films with different transmittance values.

"The aeronautical and space activities of the United States shall be conducted so as to contribute . . . to the expansion of human knowledge of phenomena in the atmosphere and space. The Administration shall provide for the widest practicable and appropriate dissemination of information concerning its activities and the results thereof."

—NATIONAL AERONAUTICS AND SPACE ACT OF 1958

NASA SCIENTIFIC AND TECHNICAL PUBLICATIONS

TECHNICAL REPORTS: Scientific and technical information considered important, complete, and a lasting contribution to existing knowledge.

TECHNICAL NOTES: Information less broad in scope but nevertheless of importance as a contribution to existing knowledge.

TECHNICAL MEMORANDUMS: Information receiving limited distribution because of preliminary data, security classification, or other reasons.

CONTRACTOR REPORTS: Scientific and technical information generated under a NASA contract or grant and considered an important contribution to existing knowledge.

TECHNICAL TRANSLATIONS: Information published in a foreign language considered to merit NASA distribution in English.

SPECIAL PUBLICATIONS: Information derived from or of value to NASA activities. Publications include conference proceedings, monographs, data compilations, handbooks, sourcebooks, and special bibliographies.

TECHNOLOGY UTILIZATION PUBLICATIONS: Information on technology used by NASA that may be of particular interest in commercial and other non-aerospace applications. Publications include Tech Briefs, Technology Utilization Reports and Technology Surveys.

Details on the availability of these publications may be obtained from:

SCIENTIFIC AND TECHNICAL INFORMATION OFFICE

NATIONAL AERONAUTICS AND SPACE ADMINISTRATION

Washington, D.C. 20546